

Pantograph Arc Detection of Urban Rail Based on Photoelectric Conversion Mechanism

XIAOYING YU^{1,2} AND HONGSHENG SU¹

¹College of Automation and Electrical Engineering, Lanzhou Jiaotong University, Lanzhou 730070, China

²Key Laboratory of Opto-Technology and Intelligent Control, Ministry of Education, Lanzhou Jiaotong University, Lanzhou 730070, China

Corresponding author: Hongsheng Su (shsen@163.com)

This work was supported in part by the National Natural Science Foundation of China under Grant 61867003 and Grant 51767013, and in part by the Project Supported by the Young Scholars Science Foundation of Lanzhou Jiaotong University under Grant 2015038.

ABSTRACT According to the solar-blind characteristic of the pantograph arc spectrum distribution, an arc detection method based on the photoelectric conversion mechanism for urban rail was proposed, and the design of each part of the arcing detection system was completed. Through the analysis of arc spectral distribution, the 275-285 nm band was determined as the detection characteristic waveband. The optical acquisition system located on the roof of the train collects the arc characteristic light and transmits it to the photoelectric conversion module, which converts the received optical signal into the corresponding current signal linearly. After amplification, comparison and screening in this module, the optical signal is sent to the data processing module for output display. Finally, a field test conducted on an urban rail transit line shows that this arc detection system can effectively detect the pantograph arc phenomenon and reflect the arc intensity linearly avoiding the influence from natural light, train load and train running direction.


INDEX TERMS Urban rail, pantograph arc, photoelectric conversion, arcing detection.

I. INTRODUCTION

The electric energy required by urban rail trains is obtained from the continuous sliding contact between the pantograph and the contact line [1]. During train operation, the pantograph and contact line may be offline due to the longitudinal vibration caused by the vehicle body vibration, irregularity of wheels and rail, hard point and other factors. The air gap between the pantograph and contact line is easily broken down by high voltage in the moment offline, and resulting in pantograph arc [2]. The hazards caused by pantograph arc include threatening the insulation safety of vehicle body equipment [3], making the train receiving current continuously, leading to the unstable running speed of the train [4], generating high-frequency noise, causing certain interference to the communication equipment and communication signal control system along the line [5], generating harmonics injected into the traction power supply network system, reducing the power supply quality [6], ablating the contact line, or even burning the contact wire and causes an accident [7]–[9].

The occurrence of arc has a certain randomness and is affected by the surrounding environment, electric field, mag-

netic field, air flow field, temperature field and other multi-physics fields [10]. It is very difficult to achieve an accurate prediction of the arc. Therefore, finding an appropriate method to realize the real-time arcing detection can measure the quality of the relationship between pantograph and catenary system, thus providing the basis for urban rail transit pantograph-catenary coordination design, maintenance and insulation design work. The existing arc detection studies of pantograph-catenary are mainly concentrated in the field of AC electrified railway [11], [12]. according to the characteristics of arc, many detection methods have appeared, such as electrical method, thermal method, acoustic method and pressure method, but all of them have the disadvantages of high false detection and omission rate [13]. Japan and Italy applied optical detection method to detect pantograph arcs using UV (Ultraviolet) light 200-240 nm and 175-195 nm bands as the characteristic signals, respectively [14]. However, the photoelectric sensor part of the detection system was installed on the roof of the train, too close to the contact line, it would be subject to severe electromagnetic interference. Computer image processing technology has also attracted the attention of researchers in the field of arc detection. Aydin et al. Obtained arcing pictures from digital camera, and used image processing technology to check whether an arc occurred [15]. And they also proposed particle swarm based

The associate editor coordinating the review of this manuscript and approving it for publication was Xue Zhou .

arc detection on time series in pantograph-catenary system [16], but the image processing method could not distinguish whether the light points in the images from arcs or other light sources. Shize Huang et al. Proposed a neural network-based arc detection and recognition method, based on the CNN method, the arc elements of arc image were extracted and judged [17], but this method could not distinguish whether the outliers produced by the system were caused by CNN model errors or by sharp sparks.

Different from the 27.5 kV power supply mode of AC electrified railways, urban rail use DC 1500V power supply generally [6]. The AC and DC pantograph arc current signals are quite different from each other, the AC pantograph arc current signal is periodic and presents a completely different state from DC [1]. Therefore, the applicability of the existing AC arc detects method in DC arc needs to be further verified. Moreover, the existing arc detection system can only detect whether the arc phenomenon occurs, but cannot accurately quantify the arc intensity [17]. Based on this, a UV method for urban rail arc detection system based on photoelectric conversion mechanism is designed in this paper. Its arc light acquisition system can collect UV light signals in the solar waveband between 275-285 nm, and convert them into an equal proportion of the current signal by PMT (Photomultiplier tube). At the same time, the number, rate, duration, intensity and position of arcs can be calculated by combining the location and speed measurement data.

In this paper, the spectral characteristics of pantograph arc and the feasibility of using solar blind method in the arc detection system are analyzed in the section of "Principle of pantograph arc detection", and the relationship between the PMT output photocurrent and arc intensity in the photoelectric conversion process is deduced. In the part of "Arc detection system structure", the optical acquisition system, photoelectric conversion module and the data processing module are designed. In the "Test" section, the arc detection system is applied to an urban rail transit line, the process and conditions of the test are explained. Finally, the experimental results and analysis are given in the section of "Results and discussion", and the conclusion is given at the end.

II. PRINCIPLE OF PANTOGRAPH ARC DETECTION

The locomotive obtains electricity by means of continuous sliding contact between the pantograph and the contact line. In order to ensure continuous contact, a certain pressure should be maintained between the pantograph and contact line, when offline occurs, the voltage difference between pantograph and contact line increases sharply, resulting in the breakdown of the gas between them, which causes the gas discharge, forms a cylindrical gas with extremely high temperature and strong luminescence, that is arc [18]. The electrons or ions in specific materials will be generated along with light at specific wavelengths in the process of energy level transitions from a high energy level to low [19]. As the offline distance increases, the arc is stretched, and when the energy absorbed by the arc is not enough to keep it

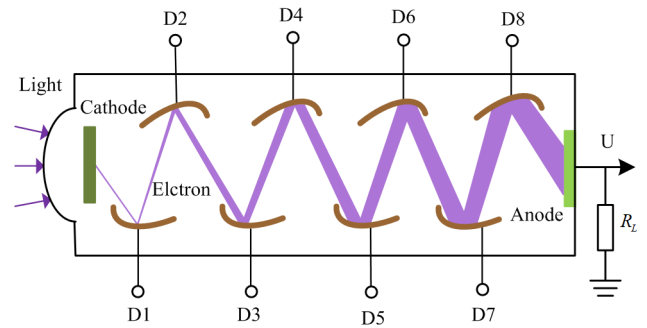


FIGURE 1. Structure and principle of PMT.

burning, the arc is extinguished [20]. The photometric method identifying and measuring the arc adopted in this paper uses the luminous characteristics of the arc, so the extracted light characteristic quantity should be able to avoid the influence of natural light in the environment.

A. PRINCIPLE OF SOLAR-BLIND ARCING DETECTION

UV wavelength in sunlight distributes in 10-400 nm, only the near UV (300-400 nm) can reach the surface of the earth, whereas the vacuum UV (10-200 nm) and medium UV (200-300 nm) are strong absorption by oxygen ions and ozone in the process of transmission. As a result, natural light at 10 to 300 nm UV is almost non-existent near the earth's surface, this band is known as the "solar blind" [21].

Our team has conducted a spectrum analysis experiment of the pantograph-contact line arcing in the laboratory, and we found that there is a certain amount of the UV bands below 300 nm in the arc spectrum, among which the radiation intensity of 275-285 nm band accounted for a stable proportion in the whole arc spectrum, it could reflect the magnitude of arc intensity [22]. At the same time, it meets the requirements of the arc detection band range in the international standard IEC 62487-2017 [23]. Therefore, using 275-285 nm as the characteristic band to measure the pantograph arc intensity of the urban rail can avoid the interference of natural light.

B. PRINCIPLE OF PMT ARCING DETECTION

This method is to convert optical signals into electrical signals and judge the arc intensity by its trend. The photoelectric element used in this system is PMT, which consists of the photocathode, focusing electrode, secondary emission multipliers and anode. It can convert the UV signal received by its cathode into corresponding electrical pulse signal and output through the anode. The working principle and equivalent circuit of PMT are shown in Fig. 1 and Fig. 2.

The cathode of PMT will emit photoelectrons after being irradiated with UV light, and the photoelectrons will be accelerated and focused in the electric field between the electrodes, thus bombards the multiplier pole at a high speed, then the multiplier produces secondary electron emission, which increases the number of electrons by several times. After several multipliers, the number of electrons increases

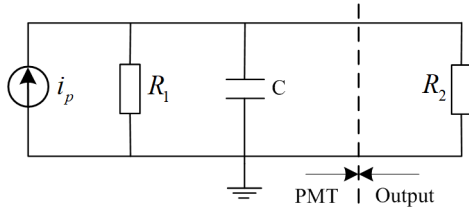


FIGURE 2. PMT equivalent circuit.

sharply, and finally is collected by the anode to form the anode current. In Fig. 2, U is the output voltage of anode, R and C represent the equivalent resistance and capacitance respectively.

The process in which PMT converts the incident optical radiation energy to the cathode into photocurrent and outputs it from the anode is called the photoelectric conversion process, use $P(t)$ to express the UV light power of the incident light radiation received by PMT. $i(t)$ to represent the output photocurrent, then their relationship can be expressed as [24],

$$P(t) = dE_R/dt = hv(dN_1/dt) \quad (1)$$

$$i(t) = dq/dt = e(dN_2/dt) \quad (2)$$

where, h is Planck's constant, ν denotes the UV frequency, N_1 is the number of photons incident at the cathode, N_2 is the number of electrons out the elementary charge, q represents photogenic charge, E_R is the incident light energy received by PMT, e is the elementary charge. According to (1) and (2), it can be obtained that,

$$i(t) = \frac{e}{hv} \frac{dN_2/dt}{dN_1/dt} P(t) \quad (3)$$

As $\eta = (dN_2/dt)/(dN_1/dt)$ is the quantum efficiency of the PMT, it represents the ratio of photons absorbed number by PMT to the number of electrons excited, which is a function of physical properties, Then (3) can be written as,

$$i(t) = (e\eta/hv)P(t) \quad (4)$$

When the light source and the environment are fixed, in (4), e , η , h , and ν are constant, let $A = e\eta/hv$, then,

$$i(t) = AP(t) \quad (5)$$

It can be seen from (5) that the photocurrent $i(t)$ output by PMT is proportional to the incident light power $P(t)$ received.

According to (1), the relationship between the light energy E_R received by the PMT cathode and the light power $P(t)$ is as follows,

$$E_R \propto \int_{t_1}^{t_2} P(t)dt \quad (6)$$

As the propagation of optical signals in the air is attenuated, μ is the absorption coefficient of PMT, k is the air absorption coefficient, L is the distance between the signal receiving point and the contact point of the pantograph-contact line, ρ is the air density. Then the relationship between the light

energy released by the arc E_S and the light energy received by the PMT cathode E_R is as follows [25],

$$E_R = \mu e^{-k\rho L} E_S \quad (7)$$

According to (6) and (7), it can be obtained that,

$$\int_{t_1}^{t_2} P(t)dt \propto \mu e^{-k\rho L} E_S \quad (8)$$

The electrical energy of arc discharge E_c and the light energy emitted by arc discharge E_S satisfy the following relationship [24],

$$\eta_l = E_S/E_c \quad (9)$$

where, η_l is the luminous efficiency, which is related to the dielectric characteristics, electric field intensity, electrode spacing, environment and other factors, and U represents the peak voltage of the initial discharge of the arc. Then, the relationship between E_c and the arc discharge Q is as follows [26],

$$E_c = UQ/2 \quad (10)$$

According to (8), (9), and (10), it can be obtained that,

$$\int_{t_1}^{t_2} P(t)dt \propto \mu\eta_l e^{-k\rho L} UQ/2 \quad (11)$$

In (11), L , μ , k , ρ , η_l and U are constants, let $B = \mu\eta_l e^{-k\rho L} U/2$, then,

$$\int_{t_1}^{t_2} P(t)dt \propto BQ \quad (12)$$

It can be seen from (5) and (12) that the optical power $P(t)$ received by PMT is proportional to the optical current output $i(t)$, and it is also proportional to the arc discharge Q , therefore, $i(t)$ is proportional to Q , so it is reasonable to judge the arc discharge intensity by detecting the output current from PMT.

III. STRUCTURE OF PANTOGRAPH ARC DETECTION SYSTEM

The pantograph arc detection system is mainly composed of three parts, an arc light acquisition system installed on the roof of the train, and a photoelectric conversion module and data processing module installed in the control room. The structure diagram is shown in Fig. 3.

When arc occurs, only 275-285 nm UV band in the arc can pass through the light acquisition system and be imaged on the end face of the fiber, then the UV fiber transmits the optical signal to the photoelectric conversion module. After the PMT converts the incident light signal into an electrical signal, it is sent to the data processing module, at the same time, the positioning and speed measurement systems provide basic data of the locomotive to locate the arc occurrence point, store and record the relevant data.

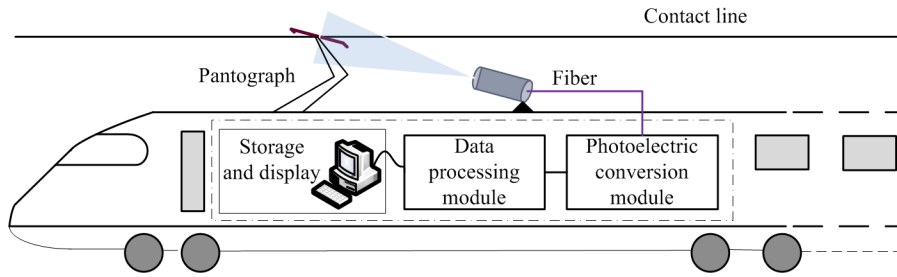


FIGURE 3. Structure of pantograph arc detection system.

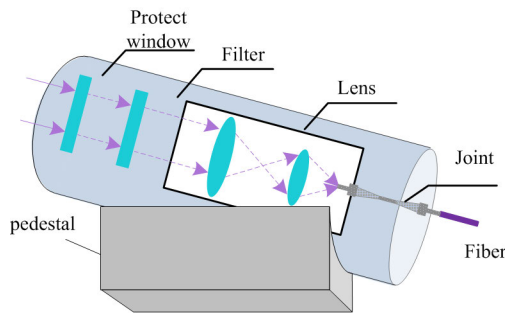


FIGURE 4. Structure of arc light acquisition system.

A. ARC LIGHT ACQUISITION SYSTEM

This arc light acquisition system should meet two requirements, first, be able to collect UV light signals in the characteristic band of 275-285 nm in the arc light, and prevent other band light signals from entering, second, the collected characteristic optical signals can be transmitted to the photoelectric conversion module for processing without loss. The structure of arc light acquisition system designed in this paper is shown in Fig. 4.

the arc light acquisition system is mounted on the roof of the train at an angle of 25°, and the mounting angle is adjustable. To satisfy the first requirement above, a narrow-band filter with a central wavelength of 280 nm and a bandwidth of 10 nm is installed at the front of the lens, at the same time, an anti-reflection coating is added to the glass element in order to reduce the light loss caused by the reflection of the surface of the glass element. After the optical signal passes through the lens group, it enters the end face of the UV fiber at the focal point and is transmitted to the photoelectric conversion module through the optical fiber for further processing, so it satisfies the second requirement.

The design of optical parameters is related to the installation position of the optical acquisition system. Considering the different arrangement of equipment on the roof of the train, this paper designs the optical parameters for the three distance schemes of the horizontal distance between the light acquisition system and the arc point, 3 m, 4 m, and 5 m. Since the vertical distance between the contact point of the urban rail contact line and the roof is small, the optical parameters

TABLE 1. Basic optical parameters of arc light acquisition system.

Parameter	<i>u</i> (m)	<i>v</i> (mm)	<i>f</i> (mm)	<i>D</i> (mm)
Value	3	18.75	18.63	8.47
	4	25.00	24.84	11.29
	5	31.25	31.06	14.11

of the arc light acquisition system can be designed according to the object distances of 3 m, 4 m, and 5 m.

The design target is that, arc with a diameter of 400 mm can be transmitted to the next module by an optical fiber with a diameter of 2.5 mm after passing through the optical system. The distance between the arc and the optical system is 3 m, 4 m and 5 m respectively, and the coupling angle of the end face of the optical fiber is 25°. The optical parameters of the imaging system are designed for three range schemes. When the image lens is equivalent to ideal, according to the design objective, the numerical aperture NA of the imaging system is limited as

$$NA = \sin(25^\circ/2) = 0.22$$

Beams larger than this NA will not be coupled into the fiber. The magnification β of an ideal lens imaging system is

$$\beta = 400/2.5 = 160$$

The image distance *v*, focal length *f*, and the effective optical aperture *D* of the three object distance *u* schemes can be calculated according to (13)-(15). And the results are shown in Table 1. When the optical acquisition system is installed at different positions (*u* is different), the fixed position of the end of the UV fiber depends on the value *f* in Table. 1, while the lens size depends on the value *D*.

$$v = u/\beta \tag{13}$$

$$1/f = 1/u + 1/v \tag{14}$$

$$f = D \times NA \tag{15}$$

B. UV PHOTOELECTRIC CONVERSION MODULE

The task of the UV photoelectric conversion module is to convert the characteristic band light signal transmitted from the optical fiber into an electric signal, that can reflect the

TABLE 2. Parameter of PMT (R9880U-210).

Parameter	Value	Parameter	Value	
Type	High Q.E.	Cathode	Shape	round
Size	Dia.16 mm		Material	Ultra bialkali
Number of multiplier poles	10		Size	Dia.8 mm
Structure of multiplier poles	Metal channel		Sensitivity (minimum)	100 A/lm
Long wavelength limit	700 nm	Sensitivity (typical)	135 A/lm	
Shortwave limit	230 nm	Anode	Sensitivity (minimum)	100 A/lm
Peak wavelength	350 nm		Sensitivity (typical)	270 A/lm
Mean anode current	0.1 mA	Time response	Rise time	0.57 ns
Gain	2.0×10 ⁶		Transit time	2.7 ns

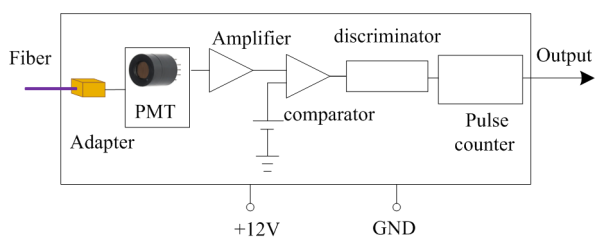


FIGURE 5. Structure of photoelectric conversion module.

arc intensity and output it to the next module. The key of the module design is as follows:

- (1) The module can convert optical signals into electrical signals, the photoelectric conversion element adopted is sensitive to the optical signals at 275-285 nm band and the response curve is close to linear within the band range.
- (2) Since the electrical signal directly output by PMT is very weak, it is susceptible to interference from noise signals in the working environment. As a direct detection signal, the detection result would be inaccurate, so corresponding measures should be taken to identify and extract valid signals.
- (3) The module should have a counting function that can count the number of pulses of the PMT anode output signal to determine the number of arcs.

After comprehensive consideration, R9880U-210 type PMT was selected. The quantum efficiency of R9880U-210 has good linearity when the wavelength of incident light distributed at 275-285 nm, and it also has the advantages of light weight, high mechanical strength, high cathode sensitivity and gain. The main characteristics of R9880U-210 PMT are as Table.2.

The structure of the photoelectric conversion module is shown in Fig. 5.

In order to solve the problem that the output electrical signal from PMT is weak and vulnerable to interference, a low noise preamplifier is designed into the module to amplify the weak electrical signal with noise. In order to filter out low and high amplitude impulse noise in the environment, comparators and discriminators are designed. By selecting the first and second levels of the discriminator reasonably, low amplitude noise pulses, such as thermionic noise pulses and amplifier noise pulses in the multiplier system, as well

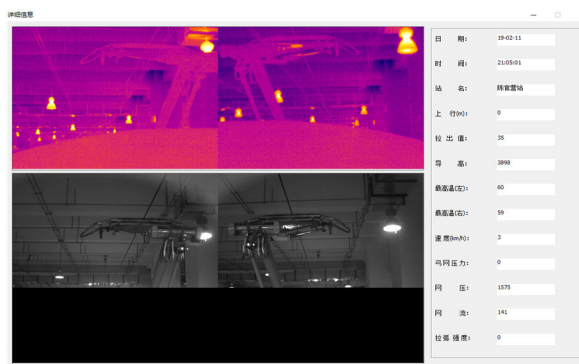


FIGURE 6. Interface display.

as high amplitude of gas fluorescence caused by cosmic rays can be eliminated, so as to improve the signal-to-noise ratio of the detection results. To realize arc counting, a pulse counting unit is designed after the discriminator to record the TTL level signal output by the discriminator.

C. DATA PROCESSING MODULE

The main task completed by the data processing module is to collect the arc information transmitted by the photoelectric sensor module and process the arcing information in combination with the data of the train positioning system GPS, TAX box and speed measuring system. It can output the location, time, duration, intensity and train running speed of arcs. At the same time, the arcing rate, arcing curve, arcing time and maximum arcing duration in the running section should be given.

The data processing part is implemented by industrial embedded computer with strong anti-interference ability. In order to achieve fast data acquisition, the system adopts the Altai 2812 data acquisition card based on USB bus, which can be directly connected to the USB interface of the computer, and it is convenient to insert and remove. The signal processed by the sensor module is transmitted to the integrated processing system of the upper computer, The system analyzes the data, calculates the arcing rate, arcing time, arcing intensity and other parameters, and combines with other monitoring information of the catenary to accurately

TABLE 3. Test conditions of arc detection.

Test No.	Time	Time of duration (min)	Train load condition	Train running direction	Average speed of train (km·h ⁻¹)	Maximum instantaneous speed of train (km·h ⁻¹)	Average station time (min)
1	Day time	45'03"	Full load	Up	34.5	78.6	1
2	Day time	45'18"	Full load	Down	34.3	77.5	1
3	Night	44'31"	No load	Up	34.9	79.4	1
4	Night	45'42"	No load	Down	34.0	76.9	1

TABLE 4. Operation conditions and arc burning conditions of sections 4, 5, and 14.

Section NO.	Section length (m)	Test NO.	Running time (s)	Average speed of train (km·h ⁻¹)	Maximum instantaneous speed of train (km·h ⁻¹)	Arcing rate (%)	Number of arcs	Total arc duration (ms)	Maximum arc duration (ms)
4	2086.49	1	216.41	34.7	78.4	0.92	8	1990	393
		2	218.94	34.3	78.0	0.71	8	1554	306
		3	215.17	34.9	79.6	0.88	7	1721	395
		4	222.18	33.8	77.9	0.64	7	1421	289
5	2012.66	1	208.74	34.7	78.6	0.56	5	1168	333
		2	211.79	34.2	77.4	0.34	4	720	253
		3	205.25	35.1	79.9	0.41	3	841	397
		4	211.17	34.3	76.8	0.28	5	591	192
14	1416.36	1	146.06	34.9	78.8	0.76	4	1110	430
		2	148.19	34.4	77.9	0.68	4	1007	391
		3	144.82	35.2	80.1	0.64	5	926	291
		4	154.47	33.0	78.0	0.60	4	927	355

TABLE 5. Arcing data of test 1.

Section NO.	Arcing NO.	Distance from the last stop (m)	Arc duration (ms)	Current signal (A)	Number of photons	Train speed (km·h ⁻¹)	Train condition
4	1	87	393	15.3	511.	17.6	Accelerating
	2	114	208	13.4	440.	34.5	Accelerating
	3	261	298	16.5	558	28.0	Accelerating
	4	791	153	12.3	417	75.0	constant
	5	1840	186	12.9	426	61.2	Braking
	6	1925	90	11.2	372	41.1	Braking
	7	1987	343	14.8	495	32.5	Braking
	8	2031	319	14.1	471	16.4	Braking
5	1	145	323	13.7	459	20.3	Accelerating
	2	207	96	7.6	248	25.5	Accelerating
	3	866	333	14.3	486	74.7	constant
	4	1893	290	12.1	399	46.5	Braking
	5	1901	126	7.9	262	11.4	Braking
14	1	123	157	9.5	308	17.2	Accelerating
	2	179	327	14.0	462	27.6	Accelerating
	3	1241	430	15.7	518	64.0	Braking
	4	1302	196	11.9	392	14.2	Braking

locate the arc occurrence location, and finally forms a report and test report output, and the interface display and output statements are shown in Fig.6. and Fig.7.

IV. TESTS

In order to verify whether the system can detect the arcing phenomenon and its intensity, the arcing detection system is

installed on a train in an urban rail transit line with its object distances 4 m to carry out tests. This urban rail transit line is officially opened in June 2019, with a total length of 25.9 km, 20 stations and 19 sections. The installation state and output interface of the device are shown in Fig. 8.

Four arc detection tests were conducted on the train, and the train’s running speed, running direction, load status and

ID	ZhCur	Zha...	ZhN...	szZh...	ISudu	szTime	lMlege	iGh	iMax...	Max...	lMA...	MA...	MA...	MA...	szCh...	Lc1	IGD1	Lc2	IGD2	iArc	lWY1	lWY2	lWL1	lWL2
0	1	0	1	陈富... 1	19-0...	0	0	58	74	135	57	111	148		-240	5050	0	0	0	1587	0	61	0	
1	1	1	1	陈富... 2	19-0...	0	0	58	80	128	57	120	142		-399	4945	0	0	0	1599	0	4	0	
2	1	2	1	陈富... 2	19-0...	0	0	58	84	121	56	128	136		-376	4975	0	0	0	1600	0	3	0	
3	1	3	1	陈富... 2	19-0...	0	0	57	88	116	56	134	131		-393	4951	0	0	0	1599	0	3	0	
4	1	4	1	陈富... 2	19-0...	0	0	57	92	112	55	140	126		-170	4988	0	0	0	1596	0	18	0	
5	1	5	1	陈富... 3	19-0...	0	0	57	95	107	55	146	122		60	3810	0	0	0	1594	0	42	0	
6	1	6	1	陈富... 3	19-0...	0	0	56	98	103	55	151	119		-110	4984	0	0	0	1598	0	43	0	
7	1	7	1	陈富... 4	19-0...	0	0	56	101	100	54	155	115		-88	5028	0	0	0	1595	0	24	0	
8	1	8	1	陈富... 4	19-0...	0	0	56	103	97	54	159	113		35	3842	0	0	0	1600	0	4	0	
9	1	9	1	陈富... 4	19-0...	0	0	56	105	94	54	162	110		19	3860	0	0	0	1600	0	4	0	
10	1	10	1	陈富... 4	19-0...	0	0	55	106	93	52	166	108		20	3868	0	0	0	1600	0	4	0	
11	1	11	1	陈富... 4	19-0...	0	0	56	109	90	52	168	105		50	3843	0	0	0	1605	0	-2	0	
12	1	12	1	陈富... 3	19-0...	0	0	55	110	88	52	171	104		65	3794	0	0	0	1599	0	4	0	
13	1	13	1	陈富... 1	19-0...	0	0	55	111	86	52	173	102		27	3876	0	0	0	1600	0	4	0	
14	1	0	1	陈富... 3	19-0...	0	0	60	367	238	59	352	264		35	3898	0	0	0	1575	0	141	0	
15	1	1	1	陈富... 5	19-0...	0	0	56	334	274	59	336	234		-165	3820	0	0	0	1595	0	34	0	
16	1	2	1	陈富... 5	19-0...	0	0	54	116	80	59	326	213		28	3897	0	0	0	1599	0	5	0	
17	1	3	1	陈富... 5	19-0...	0	0	59	296	174	59	315	195		-363	4955	0	0	0	1600	0	5	0	
18	1	4	1	陈富... 5	19-0...	0	0	61	284	160	59	308	181		-37	3851	0	0	0	1600	0	5	0	
19	1	5	1	陈富... 5	19-0...	0	0	61	273	150	59	302	171		71	3802	0	0	0	1601	0	4	0	
20	1	6	1	陈富... 5	19-0...	0	0	60	264	140	59	296	161		48	3850	0	0	0	1600	0	4	0	
21	1	7	1	陈富... 5	19-0...	0	0	60	255	133	58	293	155		25	3839	0	0	0	1600	0	5	0	
22	1	8	1	陈富... 5	19-0...	0	0	60	248	126	59	288	146		20	3909	0	0	0	1600	0	5	0	
23	1	9	1	陈富... 5	19-0...	0	0	60	242	121	59	285	140		12	3882	0	0	0	1600	0	4	0	
24	1	10	1	陈富... 4	19-0...	0	0	59	237	116	58	282	135		13	3890	0	0	0	1601	0	5	0	
25	1	11	1	陈富... 4	19-0...	0	0	59	232	111	58	280	131		15	3901	0	0	0	1600	0	4	0	
26	1	12	1	陈富... 4	19-0...	0	0	59	227	107	57	278	126		3	3854	0	0	0	1599	0	4	0	
27	1	13	1	陈富... 4	19-0...	0	0	59	224	104	57	276	123		66	3799	0	0	0	1600	0	4	0	
28	1	14	1	陈富... 4	19-0...	0	0	59	220	100	56	274	119		62	3795	0	0	0	1601	0	5	0	
29	1	15	1	陈富... 4	19-0...	0	0	58	217	97	56	272	116		31	3828	0	0	0	1598	0	5	0	
30	1	16	1	陈富... 4	19-0...	0	0	58	214	95	54	270	113		-64	4969	0	0	0	1600	0	4	0	
31	1	17	1	陈富... 4	19-0...	0	0	58	211	92	55	269	111		59	3847	0	0	0	1600	0	4	0	
32	1	18	1	陈富... 4	19-0...	0	0	58	209	90	54	268	109		-4	3847	0	0	0	1600	0	4	0	
33	1	19	1	陈富... 4	19-0...	0	0	57	207	88	53	267	107		-3	3866	0	0	0	1600	0	4	0	
34	1	20	1	陈富... 4	19-0...	0	0	57	205	86	52	266	104		83	3791	0	0	0	1600	0	4	0	
35	1	21	1	陈富... 4	19-0...	0	0	56	203	84	52	265	103		67	3802	0	0	0	1599	0	4	0	
36	1	22	1	陈富... 4	19-0...	0	0	57	201	83	52	264	101		-422	4943	0	0	0	1601	0	4	0	
37	1	23	1	陈富... 4	19-0...	0	0	56	199	81	51	285	142		-183	5040	0	0	0	1601	0	3	0	
38	1	24	1	陈富... 4	19-0...	0	0	54	198	80	51	282	136		-78	3924	0	0	0	1598	0	4	0	
39	1	25	1	陈富... 4	19-0...	0	0	55	197	79	53	1	126		-427	4961	0	0	0	1594	0	24	0	
40	1	26	1	陈富... 4	19-0...	0	0	54	228	108	52	14	122		-2	3878	0	0	0	1598	0	19	0	
41	1	27	1	陈富... 4	19-0...	0	0	54	224	104	51	24	119		32	3826	0	0	0	1599	0	4	0	
42	1	28	1	陈富... 4	19-0...	0	0	53	220	101	51	35	116		66	3795	0	0	0	1600	0	4	0	
43	1	29	1	陈富... 4	19-0...	0	0	52	217	98	54	368	264		-4	3865	0	0	0	1600	0	5	0	

FIGURE 7. Output statements.

speed were all different in each test. The tests conditions are shown in Table.3.

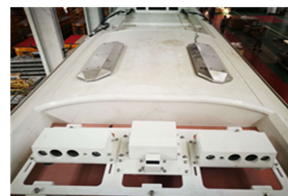
Specific arc data of the above three sections are selected for analysis, and the detected arc data are listed in Table. 5-8.

Under basically same test conditions, if a high degree of consistent arcing rate detection result can be obtained during repetitive tests, it can be proved that the system has high reliability. Due to the different test conditions and the arcing phenomenon has a certain randomness, the test results cannot be completely consistent. However, as long as the arcing rate change trends in the 19 sections obtained from the 4 tests are similar, it can be explained that the arcing detection system can effectively detect the pantograph arc phenomenon without being affected by external conditions. Arc ratio N_Q is an important index [23], and its calculation formula is as follows,

$$N_Q = \left(\sum_{i=1}^n t_i \right) / t_t \times 100\% \quad (16)$$

In (16), t_i represents the duration of the i^{th} arc whose duration exceeds 1 ms in the section under test (the influence of arc discharge less than 1 ms can be ignored), t_t represents the total measured time of the section, that is, the total running time of the train in the section [23].

From the foregoing theoretical analysis, it can be seen that the current output by the PMT $i(t)$ in the photoelectric conversion module is proportional to the amount of arc discharge



(a) Equipment on the roof



(b) Equipment in the control room

FIGURE 8. Tests equipment installation and output state.

Q , it can accurately reflect the intensity of the arc. However, at the moment arc occurs, there is no auxiliary equipment can detect Q , therefore, it is impossible to verify the correctness of arc strength by the relationship between $i(t)$ and Q , but according to (1), it can be known that,

$$N = \left(\int_{t_1}^{t_2} P(t)dt \right) / hv \quad (17)$$

That is, the number of photons received by the PMT photocathode N is proportional to the incident light power $P(t)$, considered (12) that N is proportional to Q . Therefore, in the tests, a photon counter is added to the photoelectric conversion module to measure the number of photons received by the cathode when arc occurs, and verify whether the number of photons N is proportional to the output current $i(t)$ of PMT. If so, it means that the output current $i(t)$ of PMT is

TABLE 6. Arcing data of test 2.

Section NO.	Arcing NO.	Distance from the last stop (m)	Arc duration (ms)	Current signal (A)	Number of photons	Train speed (km·h ⁻¹)	Train condition
4	1	87	306	15.2	501	12.6	Accelerating
	2	114	103	12.1	416	24.5	Accelerating
	3	261	244	14.6	498	51.0	Accelerating
	4	791	94	11.6	373	75.3	constant
	5	1840	206	12.4	410	64.2	Braking
	6	1937	227	14.3	469	39.1	Braking
	7	1987	275	15.1	511	32.5	Braking
	8	2030	99	12.3	418	6.4	Braking
5	1	145	209	13.2	436	13.3	Accelerating
	2	207	136	11.4	388	24.5	Accelerating
	3	1894	253	14.0	464	46.5	Braking
	4	1900	122	10.1	344	10.4	Braking
14	1	123	102	9.3	303	16.0	Accelerating
	2	180	390	13.5	461	21.6	Accelerating
	3	1241	190	11.7	399	24.0	Braking
	4	1340	325	12.9	420	9.2	Braking

TABLE 7. Arcing data of test 3.

Section NO.	Arcing NO.	Distance from the last stop (m)	Arc duration (ms)	Current signal (A)	Number of photons	Train speed (km·h ⁻¹)	Train condition
4	1	103	338	14.8	495	13.5	Accelerating
	2	134	320	14.7	490	21.5	Accelerating
	3	304	263	13.8	464	30.1	Accelerating
	4	797	159	12.6	426	76.0	constant
	5	1805	395	15.0	512	44.2	Braking
	6	1931	168	14.2	481	29.2	Braking
	7	1906	78	11.3	387	12.5	Braking
5	1	153	279	11.6	394	16.0	Accelerating
	2	236	397	14.5	449	26.4	Accelerating
	3	1956	165	9.6	318	16.0	Braking
14	1	164	193	11.9	394	20.6	Accelerating
	2	287	87	9.5	312	31.4	Accelerating
	3	1169	176	11.5	374	54.6	Braking
	4	1311	291	13.5	441	44.2	Braking
	5	1386	179	11.7	399	20.4	Braking

proportional to the discharge Q of arc. Then the output $i(t)$ of the system can correctly reflect the intensity of the arc.

V. RESULTS AND DISCUSSION

In the four tests, the arc ignition rate, total number and total duration of the 19 sections are shown in Fig. 9.

It can be seen from Fig. 9 (a) that in the 4 tests, the trend of the arcing rate detected in each section is similar, indicating that the system can effectively detect arcing under different external conditions. This is also proved by the similarity variation rule between the number of arcing times and the total arcing duration of the four tests shown in Fig. 9 (b).

Fig 9 (a) shows that, in the 4 tests, the sections with the highest arcing rate are sections 4, 5, and 14, the running

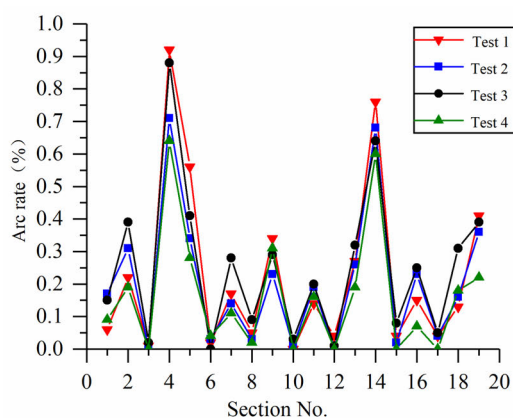
conditions of the trains in these three sections and the overall arcing conditions are shown in Table. 4.

It is found from the comparison in Table. 5-8 that, although the four tests were performed at different time periods, and the load conditions, running direction, average speed and maximum speed of the trains were all different, the mileage locations where arcing occurs are highly similar. When the train is fully loaded, the arc burning frequency, intensity and total arcing time of each section in test 1 are higher than that of test 2, however, when the train is unloaded, the arc burning frequency and burning time of test 3 are higher than that of test 4, indicating that the train running speed has a certain influence on the pantograph arc.

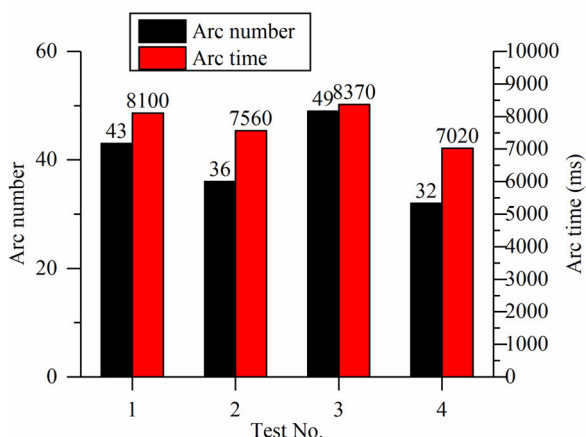
The relationship between the number of photons collected in the 4 tests and the current signal output of the photoelectric

TABLE 8. Arcing data of test 4.

Section NO.	Arcing NO.	Distance from the last stop /m	Arc duration (ms)	Current signal(A)	Number of photons	Train speed (km·h ⁻¹)	Train condition
4	1	88	209	13.1	433	15.4	Accelerating
	2	116	228	13.4	440	20.1	Accelerating
	3	261	289	14.1	483	31.0	Accelerating
	4	834	84	9.2	301	70.2	constant
	5	1840	192	12.9	435	54.0	Braking
	6	1949	131	10.4	324	29.1	Braking
	7	1988	288	14.0	475	12.4	Braking
5	1	145	49	9.2	306	15.3	Accelerating
	2	314	66	11.3	370	34.7	Accelerating
	3	866	192	15.2	501	76.0	constant
	4	1799	154	13.6	456	56.5	Braking
	5	1902	130	13.4	437	15.9	Braking
14	1	139	355	15.6	526	18.4	Accelerating
	2	203	234	12.2	401	22.2	Accelerating
	3	1241	95	10.8	355	39.0	Braking
	4	1302	243	12.3	409	16.7	Braking



(a) Arcing rate of the 19 sections



(b) Number and total duration of arcing

FIGURE 9. Arcing situation in all sections.

conversion module is shown in Fig. 10. the abscissa represents the current signal output of the photoelectric conversion

module when an arc occurs, and the ordinate represents the number of photons collected.

As can be seen from Fig. 10, in the four tests, the current signal output of the photoelectric conversion module is linearly proportional to the number of photons collected. This indicates that the system can collect the optical signal of the 275-285 nm band in the arc light and convert it into current signal $i(t)$ linearly. Furthermore, it explains that the output current signal $i(t)$ of the photoelectric conversion module is proportional to the discharge Q of the arc, and the detection result of the arc detection system can correctly reflect the strength of arc.

Before this urban rail transit line was opened, similar tests were performed on this line. At that time, considering the low speed of the train, no-load, new equipment, the corresponding current of arcing output by the PMT anode was very small and difficult to detect. Therefore, a load resistor is added at the end of the PMT to convert the output current into a voltage, and then the $\int_{t_1}^{t_2} u(t)dt$ output of the PMT anode is used to measure the pantograph arc [12]. Comparing the results in this paper, it is found that although the arcing rate of the entire line and each section has increased in the recent tests, and the duration of single arc has increased, the locations of the arcs are highly consistent. This shows that this arc detection system can effectively detect the arc burning phenomenon and accurately reflect its intensity.

VI. CONCLUSION

This paper uses the solar blind characteristic of the UV band in the pantograph arc spectrum to design an arc detection system for urban rail based on the principle of photoelectric conversion. Its arc light acquisition system can collect UV light signals in the arc blind spectrum in the 275-285 nm band and transmit them to the photoelectric conversion module. The photoelectric conversion module converts the optical

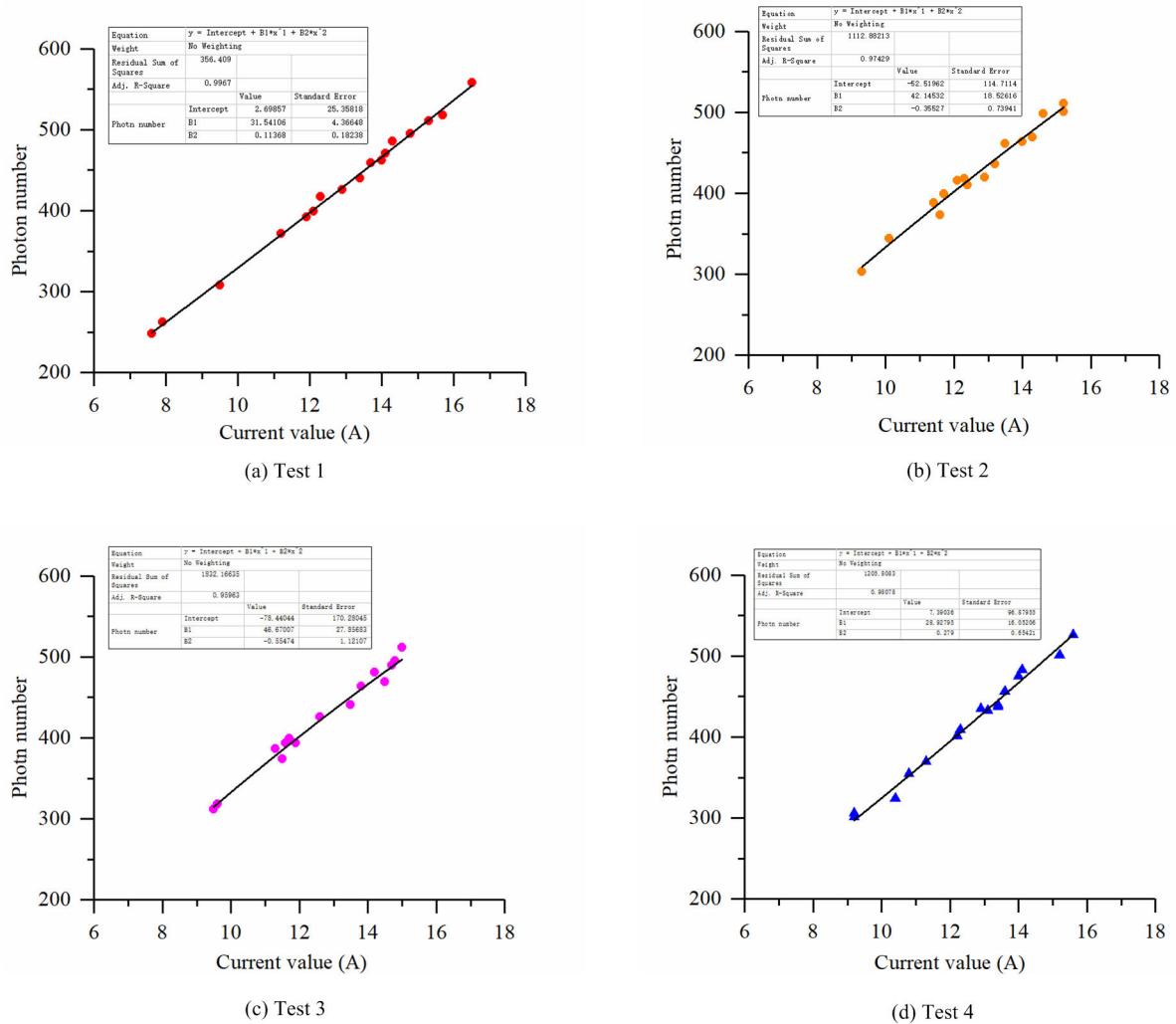


FIGURE 10. Relation between photon number and current signal output of photoelectric conversion module.

signal into an electrical signal and outputs it to a data processing module after amplification, comparison, and screening. The data processing module process output the arcing results combining the train information of the positioning and speed measurement systems.

The results of 4 arc detection tests performed on the urban rail under different conditions show that the system can effectively detect the pantograph arcing phenomenon without being affected by other factors, such as natural light, train weight, running direction, and running speed, and respond linearly to the intensity of the pantograph arc. To some extent, it can reflect the urban rail matching rationality of pantograph and catenary system. The design of this system provides a certain technical basis for the future information fusion and networked diagnosis of the pantograph-catenary system, laying a foundation for further research in this field.

REFERENCES

[1] G. Gao, X. Yan, Z. Yang, W. Wei, Y. Hu, and G. Wu, "Pantograph-catenary arcing detection based on electromagnetic radiation," *IEEE Trans. Electromagn. Compat.*, vol. 61, no. 4, pp. 983–989, Aug. 2019.

[2] Z. Liu, H. Zhou, K. Huang, Y. Song, Z. Zheng, and Y. Cheng, "Extended black-box model of pantograph-catenary detachment arc considering pantograph-catenary dynamics in electrified railway," *IEEE Trans. Ind. Appl.*, vol. 55, no. 1, pp. 776–785, Jan. 2019.

[3] S. Barmada, F. Romano, M. Tucci, and M. Raugi, "Arc detection in pantograph-catenary systems by the use of support vector machines-based classification," *IET Elect. Syst. Transp.*, vol. 4, no. 2, pp. 45–52, Jun. 2014.

[4] W. Liu, Y. Wang, T. Wang, and Z. Yang, "Influence of offline time on the characteristic of arc between pantograph and catenary," *High Voltage Eng.*, vol. 42, no. 11, pp. 3524–3532, Nov. 2016.

[5] G. Gao, J. Hao, W. Wei, H. Hu, G. Zhu, and G. Wu, "Dynamics of pantograph-catenary arc during the pantograph lowering process," *IEEE Trans. Plasma Sci.*, vol. 44, no. 11, pp. 2715–2723, Nov. 2016.

[6] X. Li, F. Zhu, R. Qiu, and Y. Tang, "Research on influence of metro pantograph arc on airport navigation system," *J. China Railway Soc.*, vol. 40, no. 5, pp. 97–102, May 2018.

[7] W. Wei, J. Wu, G. Gao, Z. Gu, X. Liu, G. Zhu, and G. Wu, "Study on pantograph arcing in a laboratory simulation system by high-speed photography," *IEEE Trans. Plasma Sci.*, vol. 44, no. 10, pp. 2438–2445, Oct. 2016.

[8] D. Ritzberger, E. Talic, and A. Schirrer, "Efficient simulation of railway pantograph/catenary interaction using pantograph-fixed coordinates," *IFAC-Papers OnLine*, vol. 48, no. 1, pp. 61–66, Jan. 2015.

[9] T. Ding, G. X. Chen, J. Bu, and W. H. Zhang, "Effect of temperature and arc discharge on friction and wear behaviours of carbon strip/copper contact wire in pantograph-catenary systems," *Wear*, vol. 271, no. 9, pp. 1629–1636, Jul. 2011.

- [10] E. Tisserand, J. Lezama, P. Schweitzer, and Y. Berviller, "Series arcing detection by algebraic derivative of the current," *Electr. Power Syst. Res.*, vol. 119, pp. 91–99, Feb. 2015.
- [11] J. Jiang, Z. Wen, M. Zhao, Y. Bie, C. Li, M. Tan, and C. Zhang, "Series arc detection and complex load recognition based on principal component analysis and support vector machine," *IEEE Access*, vol. 7, pp. 47221–47229, 2019.
- [12] X. Yu and H. Su, "Arcing detection system for pantograph-catenary system of urban transit based on voltage integral value of PMT," *J. China Railway Soc.*, vol. 41, no. 9, pp. 51–58, Sep. 2019.
- [13] Z. Wang, F. Guo, X. Feng, Y. Wang, and C. Chen, "Recognition method of pantograph arc based on current signal characteristics?" *Tran. China Electrotech. Soc.*, vol. 33, no. 1, pp. 82–91, Jan. 2018.
- [14] O. Bruno, A. Landi, M. Papi, and L. Sani, "Phototube sensor for monitoring the quality of current collection on overhead electrified railways," *Proc. Inst. Mech. Eng., F, J. Rail Rapid Transit*, vol. 215, no. 3, pp. 231–241, May 2001.
- [15] I. Aydin, M. Karakose, and E. Akin, "A new contactless fault diagnosis approach for pantograph-catenary system," in *Proc. 15th Int. Conf. MECHATRONIKA*, Dec. 2012, doi: [10.1016/j.proeng.2012.09.573](https://doi.org/10.1016/j.proeng.2012.09.573).
- [16] I. Aydin, O. Yaman, M. Karakose, and S. B. Celebi, "Particle swarm based arc detection on time series in pantograph-catenary system," in *Proc. IEEE Int. Symp. Innov. Intell. Syst. Appl. (INISTA)*, Jun. 2014, doi: [10.1109/inista.2014.6873642](https://doi.org/10.1109/inista.2014.6873642).
- [17] S. Huang, Y. Zhai, M. Zhang, and X. Hou, "Arc detection and recognition in pantograph-catenary system based on convolutional neural network," *Inf. Sci.*, vol. 501, pp. 363–376, Oct. 2019.
- [18] O. V. Van, J.-P. Massat, and E. Balmes, "Waves, modes and properties with a major impact on dynamic pantograph-catenary interaction," *J. Sound Vib.*, vol. 402, pp. 51–69, Aug. 2017.
- [19] Y. Hu, W. Wei, D. Lei, G. Gao, and G. Wu, "Experimental investigation on spectral characteristics of pantograph-catenary arc plasma," *Trans. China Electrotech. Soc.*, vol. 31, no. 24, pp. 62–70, Dec. 2016.
- [20] G. Wu, Y. Zhou, D. Lei, W. Wei, J. Wu, and G. Gao, "Research advances in electric contact between pantograph and catenary?" *High Voltage Eng.*, vol. 42, no. 11, pp. 3495–3506, Nov. 2016.
- [21] H. Zheng and T. Bai, "Development analysis and state of UV warning technology?" *Infr. Technol.*, vol. 39, no. 09, pp. 773–779, Sep. 2017.
- [22] X. Yu and H. Su, "Characteristic waveband of pantograph-catenary arcing detection system for urban rail by integral method," *J. Northwest Normal Univ. (Natural Sci.)*, vol. 55, no. 03, pp. 54–58, May 2019.
- [23] *Railway Applications Current Collection Systems-Technical Criteria for the Interaction Between Pantograph and Overhaed Contactline*, Standard IEC 62486-2017, International Electrotechnical Commission, Geneva, Switzerland, 2017.
- [24] Z. Zhang, D. Lin, X. Yu, and Y. Wang, *Principles and Techniques of Optoelectronics*. Beijing, China: Beihang Univ. Press, 1987.
- [25] J. Tang, Y. Liu, Y. Qiu, and J. Yuan, "Relationship between first integral value of signal of the optical method and charge quantity of partial quantity of partial discharge from needle-plate electrode," *High Voltage Eng.*, vol. 38, no. 01, pp. 1–8, Jan. 2012.
- [26] D. Eadie and M. Santoro, "Top-of-rail friction control for curve noise mitigation and corrugation rate reduction," *J. Sound Vib.*, vol. 293, nos. 3–5, pp. 747–757, Jun. 2006.



way and urban rail transit.

XIAOYING YU was born in China, in 1984. She received the M.S. degree in electrical engineering from Lanzhou Jiaotong University, Lanzhou, China, in 2007, where she is currently pursuing the Ph.D. degree with the School of Automation and Electrical Engineering. She is currently a Lecturer with the Electrical Engineering Department, Lanzhou Jiaotong University. Her current research interests include on-line monitoring of overhead catenary parameters of electrified rail-



HONGSHENG SU was born in Jingyuan, Gansu, China, in 1969. He received the B.S. and M.S. degrees in industrial electric automation engineering from Lanzhou Jiaotong University, Lanzhou, China, in 1992, and the Ph.D. degree in electric power system and its automation engineering from Southwest Jiaotong University, Chengdu, in 2007.

From 1992 to 2004, he was an Engineer and a Senior Engineer with the Survey and Design Institute, Lanzhou Jiaotong University. Since 2009, he

has been a Professor with the Electrical Engineering Department, Lanzhou Jiaotong University. He is the author of more than 120 articles and more than ten inventions. His research interests include power system analysis, exploration and utilization of renewable energy, and system reliability and safety analysis. He holds two patents.

Dr. Su was a member of the China Association of Automation, in 2018. He has been an Appraisal Expert of Outstanding Project Investigation and Design in China Railway Corporation, since 2015. His awards and honors include the 16th Yong Teacher Achievement Award (Gansu Normal Higher School) and the Advanced Individual Award in Scientific Research (Lanzhou Jiaotong University). He is an Associate Editor of the *Journal of Lanzhou Jiaotong University*.

• • •